J. Astrophys. Astr. (2022) 43:37
https://doi.org/10.1007/s12036-022-09817-8

TRANSIENTS

Recent advances in the study of the prompt emission of gamma-ray bursts

SHABNAM IYYANI

School of Physics, Indian Institute of Science Education and Research, 695551 Thiruvananthapuram, India.
E-mail: shabnam@iisertvm.ac.in

MS received 15 October 2021; accepted 19 January 2022

Abstract. Gamma-ray bursts are the most energetic transients occurring in the distant cosmos. They are produced by either the collapse of massive stars or the merger of compact objects like neutron stars or black holes. Currently, gamma-ray burst is the only astrophysical event successfully observed in different messengers such as gravitational and electromagnetic waves. Despite several decades of extensive observations and research, gamma-ray bursts still remain largely elusive in terms of their central engine, jet composition and radiation process. In this article, the author will review the recent observational and theoretical advancements made in the direction to resolve some of these enigmas and the future outlook.

Keywords. Gamma-ray burst—polarization—multi-messenger.

1. Introduction

Gamma-ray burst (GRB) was a serendipitous discovery by the US-military satellite-based surveillance program during 1967. This major discovery opened up a completely astounding field of astronomy and astrophysics which allowed us to observe extremely high-energy catastrophic events in the Universe in great detail.

The GRB-event consists of two main parts: (i) prompt emission which happens on a shorter timescale of a few to hundred seconds and composes of the immediate gamma-ray emission which is produced close to the burst site; (ii) afterglow emission is observed after a certain delay which happens for a longer duration of several hundreds of seconds to days and even months, and composes of emission that can be observed in multiple wavelengths ranging from radios to gamma-rays[1]. Based on the duration of the observed prompt gamma-ray emission, the GRBs are broadly classified into two main types (Kouveliotou *et al.* 1993): (i) long GRBs are those with a duration >2 s and are produced by the death of massive stars (Kawabata *et al.* 2003; Stanek *et al.* 2003; Langer *et al.* 2008), on the other hand, (ii) short GRBs are those with duration <2 s and are produced by the merger of compact objects like binary neutron stars or a neutron star – a black hole (Abbott *et al.* 2017a, b). The extreme energetics of the order of 10^{48}–10^{52} erg of these events make them the brightest explosions known to occur in the universe. They come from very distant cosmos with the measured redshifts ranging between $z = 0.009$ (Abbott *et al.* 2017a) and $z = 9$ (Cucchiara *et al.* 2011). Thus, the very distant GRBs carry information from as early as from the first stars and galaxies that were formed around 550 million years after the beginning of the Universe.

For nearly more than half a century, GRBs have been extensively observed and studied by scientists using various satellite and ground-based observatories across multiple wavelengths of electromagnetic radiation. With the advent of gravitational wave observations, currently, GRB is the only recorded astrophysical event with successful observation across both gravitational and electromagnetic waves. The

[1]The duration of the prompt gamma-ray emission is characterized by the T_{90} parameter which represents the duration during which 90% of the burst emission is recorded by the observing instrument. Thus, the T_{90} measurement is dependent on the sensitivity of the instrument in its observable energy window.

This article is part of the Special Issue on "Astrophysical Jets and Observational Facilities: A National Perspective".

Published online: 25 June 2022

GRB event is understood to be powered by a very compact source and produces highly relativistic outflow in the form of a jet. However, despite several years of extensive research, the process of radiation, the composition of the outflow, geometry of the jet, and progenitors are not well understood. The unique, non-repetitiveness and transient nature of these events make their study extremely challenging to eventually develop a generic picture of their origin.

Using the hard X-ray as well as gamma-ray observatories such as Burst and Transient Source Explorer onboard Compton Gamma Ray Observatory CGRO (Goldstein *et al.* 2013), Neil Grehels Swift (Gehrels & Swift 2004), *Fermi* gamma-ray space telescope (Meegan *et al.* 2009), etc., we have been able to detect thousands of GRBs and thereby, gather a wealth of spectral information. Currently, the spectral studies alone are insufficient to come to a conclusive understanding about various GRB properties (for a recent review please refer Kumar & Zhang 2015; Pe'er 2015; Iyyani 2018). In this respect, observables such as polarization and with the advent of multi-messenger astronomy, information from gravitational waves and neutrinos can be pivotal in arriving at an unambiguous comprehension about the physics of GRBs.

In this article, the author will review the recent advances that have been made to understand the different aspects of radiation physics using the novel technique of spectro-polarimetry, the structured jet viewing geometry and the central engine using the spectral information obtained in a wide energy range for a large sample of GRBs observed using *Fermi* and Swift gamma-ray space telescopes.

2. Current paradigm of GRB spectroscopy

Understanding the radiation process giving rise to the observed prompt gamma-ray emission has been one of the focuses of GRB spectroscopy. The GRB spectrum generally looks non-thermal and is modeled using a phenomenological function known as the Band function.[2] The competing radiation models are either the thermal (Ryde 2004; Pe'er 2008; Ryde & Pe'er 2009; Beloborodov 2011; Ghirlanda *et al.* 2013; Iyyani *et al.* 2013; Larsson *et al.* 2015; Acuner *et al.* 2020) or modified thermal (Pe'er & Waxman 2004; Beloborodov 2010; Iyyani *et al.* 2015; Ahlgren *et al.* 2015, 2019) emission coming from the jet photosphere or the various versions of optically thin synchrotron emission (Rees & Meszaros 1992; Tavani 1996; Zhang & Yan 2011; Beniamini *et al.* 2018; Burgess *et al.* 2014, 2020). In general, the low energy spectral slopes are used as a diagnostic to identify whether the observed radiation can be associated to any of the proposed theoretical spectral models. In simple synchrotron emission models, the spectral slopes $\alpha > -0.67$ cannot be produced (Preece *et al.* 1998) and this is referred to as the 'line of death' of synchrotron emission. The α distributions obtained by several GRB spectral catalog studies by BATSE, Fermi, Swift, etc., have found a significant fraction of cases with α greater than this limit. Such spectra with $\alpha > -0.67$ are most probably expected to be coming from the jet photosphere. However, by incorporating realistic jet and shock dynamics, more complex emission models have emerged such as subphotospheric dissipation models, geometrical broadening in photospheric emission, synchrotron emission in decaying magnetic fields, time-dependent cooling of synchrotron electrons, etc. These sophisticated emission models can produce a wide range of α values and thereby the investigation of low energy spectral slopes to identify the radiation process has become degenerate.

Additionally, it has been noted that due to the limitation of the forward folding technique of spectral data analysis, the burst spectra which may be found to possess α or spectral width inconsistent with the synchrotron emission model are, however, found to be consistent when the synchrotron physical model is directly tested with data (Iyyani *et al.* 2016). Such direct testing of different types of photospheric and synchrotron models with GRB spectral data have been carried out in many studies (Burgess 2014; Ahlgren *et al.* 2015, 2019; Burgess *et al.* 2020). However, in most cases, these models are statistically equally consistent with data (Iyyani *et al.* 2016; Acuner *et al.* 2020), thereby making the understanding of underlying radiation ambiguous.

There are two possible ways forward: (i) we consider a particular physical model of choice, examine its fits to data and if consistent with the data then assess if the physical implications of the model with the obtained fit results are feasible or not; (ii) we need additional constraining observables like polarization

[2]Band function consists of two power laws smoothly joined at a break. The low and high energy power-law indices are represented by α and β respectively with values as obtained in the photon counts spectrum. The peak of the spectrum in νF_ν plot is known as the Band $E_{\rm peak}$ (Goldstein *et al.* 2013; Gruber *et al.* 2014).

or gravitational wave observations which can give more information.

3. Spectro-polarimetry

The polarization property of GRBs can be a crucial observable in discerning their radiation physics and viewing geometry. Different radiation models are expected to give rise to a different range of polarization values which make their measurements significant (Gill *et al.* 2021). In Toma *et al.* (2009) and Gill *et al.* (2018) have shown that when viewed within the jet cone of GRBs with a top hat jet structure can produce low to null polarization for emission coming from direct/inverse Compton scattering involved in jet photosphere or synchrotron emission produced in random magnetic fields. On the contrary, synchrotron emission produced in ordered magnetic fields can produce high polarization ranging between 10% and 65% (Granot 2003; Toma *et al.* 2009). These discernible predictions between radiation models have been highly motivational to conduct polarization measurements in GRBs.

The polarization measurement of GRB prompt gamma-ray emission is, however, largely an unexplored field in astronomical observations. This has been because the effort is highly challenging due to the transient nature of the burst as well as the complex intricacies involved in understanding the instrument systematics and their effects. Only a few instruments, e.g., Compton imaging telescope (COMPTEL, Schönfelder *et al.* 1993) and BATSE (Paciesas *et al.* 1989) instruments onboard CGRO, Ramaty High-Energy Solar Spectroscopic Imager (RHESSI, McConnell *et al.* 2002), Imager on Board the INTEGRAL Satellite (IBIS, Forot *et al.* 2007) and Spectrometer on INTEGRAL (SPI, Kalemci *et al.* 2004; Chauvin *et al.* 2013) onboard INTEGRAL, GAmma-ray Polarimeter (GAP) onboard IKAROS (Yonetoku *et al.* 2011), Cadmium Zinc Telluride Imager (CZTI) (Rao *et al.* 2017) onboard Astrosat, and POLAR (Kole 2018) have carried out polarization measurements till date. Among the polarization measurements (Coburn & Boggs 2003; Wigger *et al.* 2004; Götz *et al.* 2009; Yonetoku *et al.* 2011, 2012; Chattopadhyay *et al.* 2017; Zhang *et al.* 2019; Sharma *et al.* 2019) that were made most of them lacked statistical significance and therefore were less convincing and did not help to constrain radiation models. However, the situation can be improved if a composite analysis and modeling of both spectrum and polarization observations of the prompt emission is carried out. The consequent improvement in our understanding of the radiation and the jet viewing geometry has been demonstrated in works such as Chand *et al.* (2018), Sharma *et al.* (2019), Sharma *et al.* (2020) where spectro-polarimetric studies combining *Fermi* and AstroSat CZTI were done. The details of these works are discussed below.

GRB 160802A was among one of the brightest GRBs observed by both *Fermi* and AstroSat CZTI. The observed high fluence ($1.04 \pm 0.08 \times 10^{-4}$ erg cm^{-2}) in the energy range 10–1000 keV enabled a constrainable polarimetric measurement across the first emission episode by AstroSat (Chand *et al.* 2018). The temporal study of the spectral parameters of the Band function fits the spectral data observed by *Fermi* revealed that throughout the first emission episode, the low energy power-law index α was found to be ≥ -0.67 (Figure 1). This, as discussed in Section 2, most likely points towards radiation originating from the photosphere. However, the measured polarization fraction was found to be high with a possible value >35% at 68% confidence interval of two parameters of interest (Chattopadhyay *et al.* 2019) which is in contradiction to what is expected from photospheric emission when observed within a GRB jet cone (Figure 1). Off-axis viewing outside the jet cone can break the symmetry of emission within the view cone ($1/\Gamma$, where Γ is the bulk Lorentz factor of the outflow) across the line of sight of the observer and lead to some net polarization fraction value. If we considered, a decaying jet structure outside a certain jet opening, as discussed in Lundman *et al.* (2014), it was shown to produce a maximum polarization fraction of 45% but with low observed energy flux. However, the extreme brightness of GRB 160802A ruled out this possibility. Thus, the spectro-polarimetric observations could be reconciled by considering a physical scenario of subphotospheric dissipation emission produced within a top hat jet structure when viewed along its edge (Chand *et al.* 2018).

Owing to the extreme brightness of GRB 160821A, a detailed spectro-polarimetric analysis was carried out using *Fermi* and AstroSat data in Sharma *et al.* (2019). The analysis results in terms of both spectrum and polarization were atypical. The main episode of the burst emission lasted for more than 100 s and exhibited a spectrum consisting of a blackbody at lower energies, in addition to the broad Band function

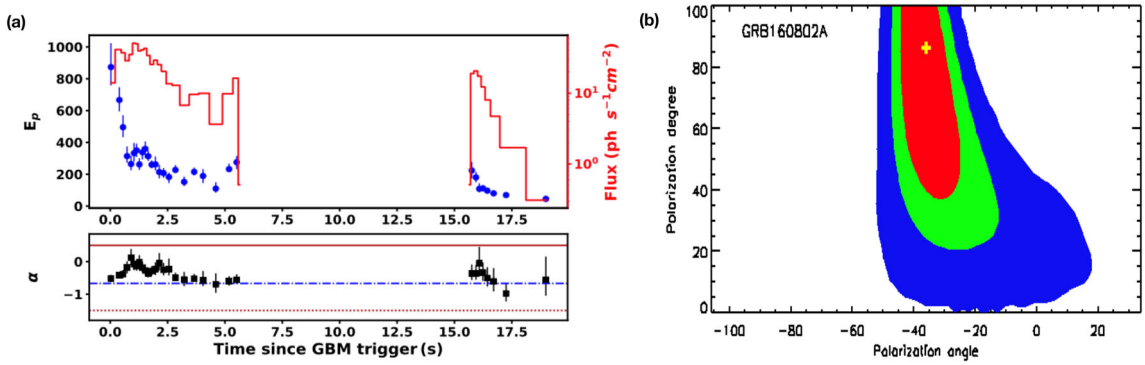

Figure 1. GRB 160802A: (a) The temporal evolution of the peak of the Band fucntion, E_p (blue circles) and the spectral slope α (black squares) obtained for the two episodes of emission are shown (Chand *et al.* 2018). (b) The 2-D histogram plot of the polarization fraction and polarization angle obtained for the burst is shown. The red, green and blue represent 68%, 90% and 99% confidence intervals of two parameters of interest; polarization fraction and polarization angle (Chattopadhyay *et al.* 2019).

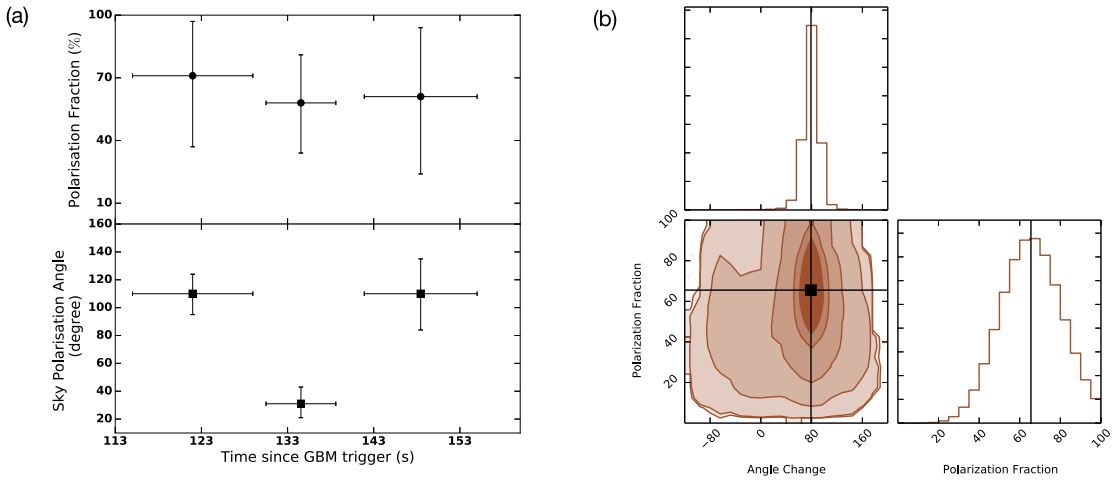

Figure 2. GRB 160821A: (a) The upper and lower panels show the polarization fraction and the respective polarization angles obtained in the three time-resolved intervals across the main emission episode, respectively. We note that though the polarization fraction remains high throughout the intervals, the polarization angle flips by nearly 90° between the time intervals. (b) Taking into account the change in polarization angle, the average polarization fraction across the emission episode is found to be $\sim 66\%$ at a statistical significance of 5.3σ. The innermost and the outermost contours on the 2-D histogram plot represent the 68% and 99.99995% (5.4σ) confidence intervals of two parameters of interest (Sharma *et al.* 2019).

with a high energy cut-off at energies greater than a few MeV. Temporally, the spectrum below the spectral peak (<800 keV) was found to remain steady ($\alpha \sim -1$) whereas the high energy end of the spectrum extending to a few hundred MeVs showed significant variation with time. Concurrent to these variations, the time-resolved polarimetry across the emission episode characterizing the rise, peak and decay phases, showed the polarization angle to swing by nearly 90° between the phases. Such a temporal variation of polarization was observed and reported at a statistical significance of 3σ for the first time (Figure 2). Due to the temporal variation in polarization, the average polarization fraction across the entire main emission episode was found to be low $<20\%$, however, after taking into account the variation in the polarization angle, a high linear polarization of $\sim 66\%$ was measured across the episode, see Figure 2 (Sharma *et al.* 2019). The high energy flux guaranteed that the burst was viewed within the jet cone and thereby the observed high polarization suggested that the radiation is synchrotron produced in magnetic fields which are ordered at the least on the angular scale of the view cone of $1/\Gamma$. The cause of the

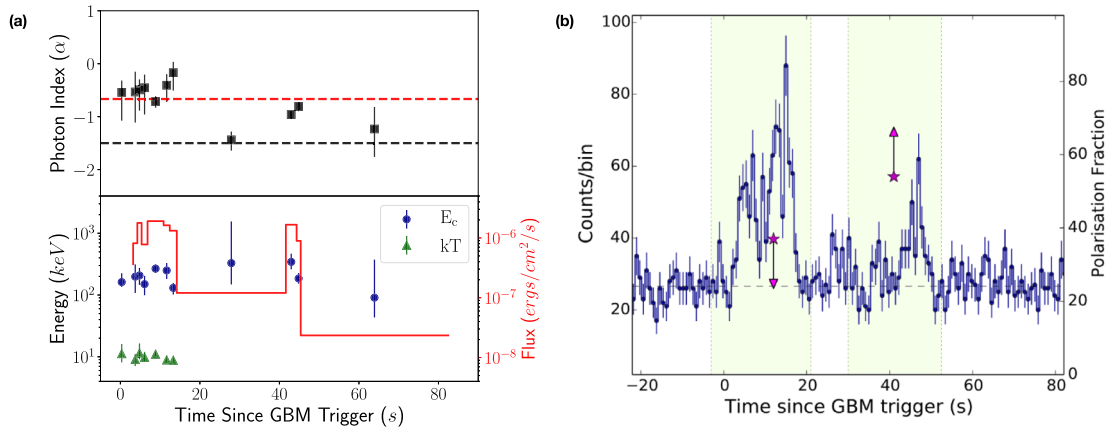

Figure 3. GRB 160325A: (a) The temporal evolution of the spectral parameters such as the power-law index (α, black squares in upper panel), the cutoff energy of the spectral model (blue circles in lower panel), i.e., power-law with exponential cuttoff, and the temperature, *kT* (green triangles in lower panel), of the blackbody function obtained for the two emission episodes are shown. The blue and red dashed horizontal lines in the upper panel represent the fast and slow cooling photon indices, $-3/2$ and $-2/3$, respectively. (b) The upper and lower limits of the polarization fractions estimated for the two emission episodes for a 1.5σ confidence interval for one parameter of interest are shown in magenta stars (Sharma *et al.* 2020).

change in polarization angle happening at small timescales of ~ 10 s within a single emission episode (or underlying multiple emission episodes), however, is unknown and calls for a more detailed study of the physics of the dynamics of GRB radiation.

GRB 160325A was a burst wherein two emission episodes separated by a certain quiescent period showed two distinct polarization properties (Sharma *et al.* 2020). The first emission episode was found to exhibit low to null polarization with a highly unconstrained polarization angle and thereby enabling us to only estimate an upper limit of polarization fraction $<37\%$ at 68% confidence level of two parameters of interest (3). This was found to be consistent with the spectral analysis which showed that the burst spectrum was largely consistent with emission coming due to subphotospheric dissipation. This was inferred based on the hard spectral slopes $\alpha > -0.67$ that were obtained for the cutoff power-law functions that were used in addition to a relatively stronger blackbody component, see Figure 3 (Guiriec et al. 2010; Iyyani *et al.* 2015). However, the second emission episode exhibited a high polarization fraction $> 43\%$ for 68% confidence interval of two parameters of interest and the spectrum was found to be only consistent with cutoff power-law function with α consistent with synchrotron emission. The X-ray afterglow observed by Swift XRT allowed us to assess that the burst is viewed within the jet cone and the radiation efficiency of the burst is low nearly 11%. If so, the varying polarization and the respective spectra observed across the two episodes suggested that the outflow is baryon dominated with a mild/passive magnetization involving large-scale ordered magnetic field lines anchored at the central engine. The first emission episode originated due to quasi-thermal Comptonisation happening at a kinetic energy dissipation site at moderate optical depths below the photosphere which leads to low polarization. On the other hand, during the second emission episode, the dissipation site had moved out into the optically thin region allowing the electrons to cool within the subdominant ordered magnetic fields producing a net polarization.

Thus, the above detailed composite modeling of the spectrum and the polarization properties of these GRBs revealed the details of the jet composition, viewing geometry, radiation model, microphysical properties such as the magnetic field configuration and its dynamics at the dissipation site with time. In future, a statistically significant sample of such studies can bring better insight into the overall physics of GRBs.

4. Energetics and central engine

The central engine powering these explosive events largely remains a mystery to date. The variability timescales of the erratic GRB light curves are found to be of the order of 30 ms and 3 ms for long and short GRBs, respectively, (MacLachlan *et al.* 2013; Golkhou & Butler 2014). The

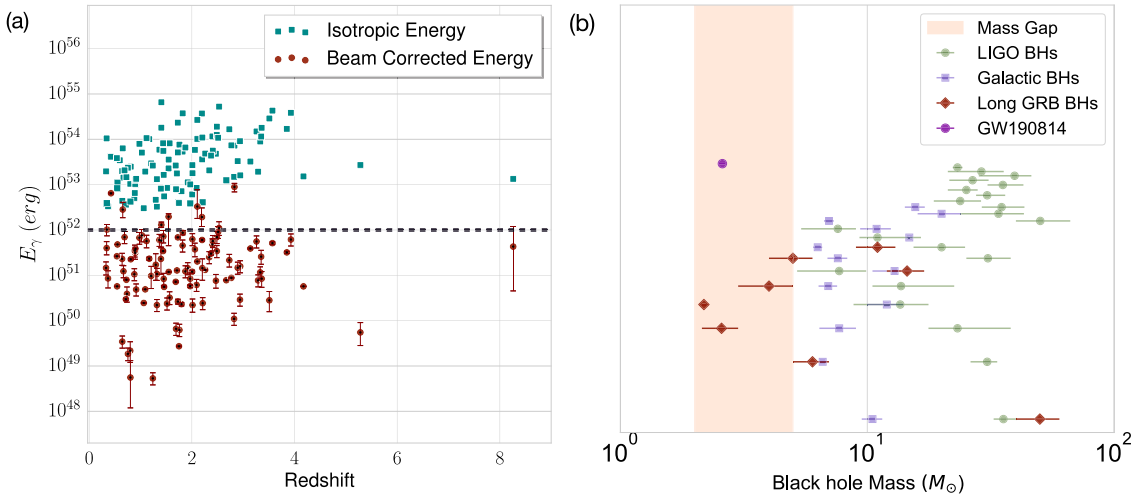

Figure 4. (a) The isotropic burst energies, $E_{\rm iso}$ (green squares), obtained for the 105 hyper-energetic GRBs are shown with respect to the respective redshift measurement made for the GRBs. The respective beam corrected burst energies, $E_{\rm jet}$, are shown in red circles. The black dashed horizontal line represents the upper limit (10^{52} erg) of magnetar rotational energy that can be channeled into the GRB jet. (b) The mass estimates of the identified black hole central engines in 8 long GRBs are shown in red diamonds. For comparison, the other known estimates of masses of black holes and the unidentified low mass object detected in GW190814 (purple circle) are also shown (Sharma *et al.* 2021).

short variability timescales suggest the source size to be of the order of 10^8–10^9 cm, thereby, pointing towards a compact source. The popular central engine models are magnetar (magnetised neutron star) (Usov 1992; Metzger *et al.* 2011) and hyper-accreting black holes (Woosley 1993; Narayan *et al.* 2001).

In general, the observance of the plateau, flares and steep decays in the X-ray afterglow lightcurves are taken as the signature of the presence of the magnetar as the GRB central engine. It is believed that these are produced due to the late time spin-down of the magnetar (Rowlinson *et al.* 2014; Sarin *et al.* 2019; Zhao *et al.* 2020). However, there have been several other studies arguing for these features to be produced by a black hole as well. Thus, overall such inferences have been largely ambiguous. One robust methodology to check for the black hole central engine is using the burst energetics (Cenko *et al.* 2011).

The magnetars are fast-spinning, highly magnetized neutron stars. The maximum rotational energy of the magnetar is given by

$$E_{\rm rot} \simeq \frac{1}{2}\, I\, \Omega^2 \approx 3 \times 10^{52}\ {\rm erg} \left(\frac{M_{ns}}{1.5\ M_\odot}\right) \left(\frac{R_{ns}}{12\ {\rm km}}\right)^2 \left(\frac{P_{ns}}{1\ {\rm ms}}\right)^{-2}. \quad (1)$$

This maximum limit of rotational energy is due to the limitation of the observed periodicity of the X-ray millisecond pulsars, P_{ns} of 1 ms (Hessels *et al.* 2006; Chakrabarty 2008; Patruno *et al.* 2017), the average mass of the millisecond pulsars are found to be $M_{ns} = 1.48 \pm 0.2\, M_\odot$ (Özel *et al.* 2012) and the respective limit on the maximum possible radius of the neutron star due to the equation state to be $R_{ns} = 12$ km. It is reasonable to consider equipartition between the different channels of lose of this rotational energy in the form of gravitational waves, magnetospheric winds and GRB jet. Thus, we find that it is largely impossible to produce burst energetics greater than $E_{\rm jet} = 10^{52}$ erg with magnetar as its central engine (Beniamini *et al.* 2017; Metzger 2017; Metzger *et al.* 2018).

Using this burst energy limit as the diagnostic in Sharma *et al.* (2021), we have probed all the 135 GRBs with known redshifts detected by *Fermi* during the years 2008–2019. First, we identified 105 hyper-energetic long GRBs with isotropic burst energies $E_{\rm iso} > 3 \times 10^{52}$ erg (Figure 4). The burst energies were calculated using the bolometric fluences that were estimated in the energy range 1 keV– 1 GeV or to the highest GeV photon that was detected. We note that no short GRB made this cut. We then estimated the beam corrected burst energetics for these GRBs

since the GRB outflow is collimated with a certain jet opening angle of θ_j (Figure 4). Finally, we identified 8 long GRBs with beam corrected total burst energy, $E_{\rm jet} > 10^{52}$ erg. All, but one, of these GRBs had significantly high energy emission (30 MeV to a few GeV) detected in *Fermi* Large Area Telescope. Thus, making them the brightest GRBs ever detected and affirmed to be powered by black holes.

There are two popular mechanisms of producing jets from a black hole: neutrino annihilation from neutrino-dominated accretion flow (Ruffert *et al.* 1997; Chen & Beloborodov 2007) and Blandford-Znajek (BZ) mechanism of extracting the rotational energy of the Kerr black holes (Lee *et al.* 2000; Tchekhovskoy *et al.* 2011). In recent simulations, it was shown that the neutrino annihilation mechanism is inefficient in producing ultra-relativistic jets (Leng & Giannios 2014). Therefore, by considering the BZ mechanism of jet production, we estimate the possible mass range of these identified GRB black hole central engines using the following relationship

$$E_{\gamma,\rm beam} = \eta 1.8 \times 10^{54}\, f_{\rm rot}(a_*)\, \frac{M_*}{M_\odot}, \qquad (2)$$

where η represents the net efficiency of converting the rotational energy of the black hole into the observed gamma-ray emission of the GRB and M_* is the mass of the black hole and

$$f(a_*) = 1 - \sqrt{(1 + \sqrt{1 - a_*^2})/2}, \qquad (3)$$

where a_* is the dimensionless black hole spin parameter which can range between 0 and 1 for non-rotating and maximally rotating black hole respectively. The η factor is considered to range between 0.4% and 14% and this includes different efficiency factors involving the maximum efficiency of BZ mechanism ($\sim$31%, Lee *et al.* 2000); black hole spins of $a^* = [0.5, 0.9]$ can convert 7–47% of the extracted BZ power into a jet and finally, the radiation efficiency estimated for the different GRBs. Using the above relation, we, thus, find the masses of the black holes to range between 2 and 60 $M_\odot$ (Figure 4).

Interestingly, we note that a fraction of these black hole mass estimates lies in the mass gap region (2–5 $M_\odot$), see Figure 4. Observationally, there have been a lack of measurements of massive neutron stars (>2 $M_\odot$) and lighter black holes <6 $M_\odot$. This study tells us that it is likely that lighter stellar-mass black holes can be created in these catastrophic events.

5. Multi-messenger astronomy and short GRBs

Albert Einstein's general theory of relativity had predicted gravitational waves which are ripples in space and time. With the launch of different gravitational wave detectors such as LIGO, VIRGO and KAGRA, across the world, scientists are now able to detect gravitational waves produced while the merging of the densest compact objects such as binary black holes, binary neutron stars and neutron star – a black hole. With the concurrent detection of electromagnetic radiation, i.e., a short GRB 170817A along with the gravitational waves, GW 170817 (Abbott *et al.* 2017a), from the merging of binary neutron stars confirmed the long-standing hypothesis that at least a class of short GRBs are produced from binary neutron star mergers. This marked the dawn of multi-messenger astronomy and currently, GRB is the only astrophysical event successfully detected across the entire range of electromagnetic radiation and now in gravitational waves.

During the gravitational wave event of GRB 170817A, an extensive followup observations across electromagnetic radiation was carried out by the X-ray space (Haggard *et al.* 2017) and ground optical, radio telescopes leading to the first conclusive observation of kilonova (Díaz *et al.* 2017; Pian *et al.* 2017) and also of an atypical afterglow emission (Kim *et al.* 2017; Haggard *et al.* 2017; Troja *et al.* 2018). The following aspects were confirmed via this event: (i) the relativistic GRB jet is viewed off-axis (Granot *et al.* 2018; Mooley *et al.* 2018a, b) and (ii) the jet has some structure beyond certain core region (Alexander *et al.* 2018; Resmi *et al.* 2018). This finding immediately implies that the observed GRB prompt emission spectra would significantly depend on the kind of jet structure and dynamics at that particular viewing angle. This prompted us to analyze the spectra of short GRBs with this perspective in Iyyani & Sharma (2021).

The 61% of the α of the Band function spectral fits done to the time-integrated emission of *Fermi* detected short GRBs are found to possess values > -0.67 and among them 69% are found to possess steeper $\beta < -2.5$ suggesting that the overall spectrum is quite narrow pointing towards emission coming from the jet photosphere, see Figure 5. In Lundman *et al.* (2013), the authors studied in detail the different kinds of spectral shapes that can be expected at different viewing angles, from a non-dissipative photosphere of a jet with a structure such that the Lorentz factor of the jet decreases as a power-law outside a jet core, θ_c, whereas, the burst

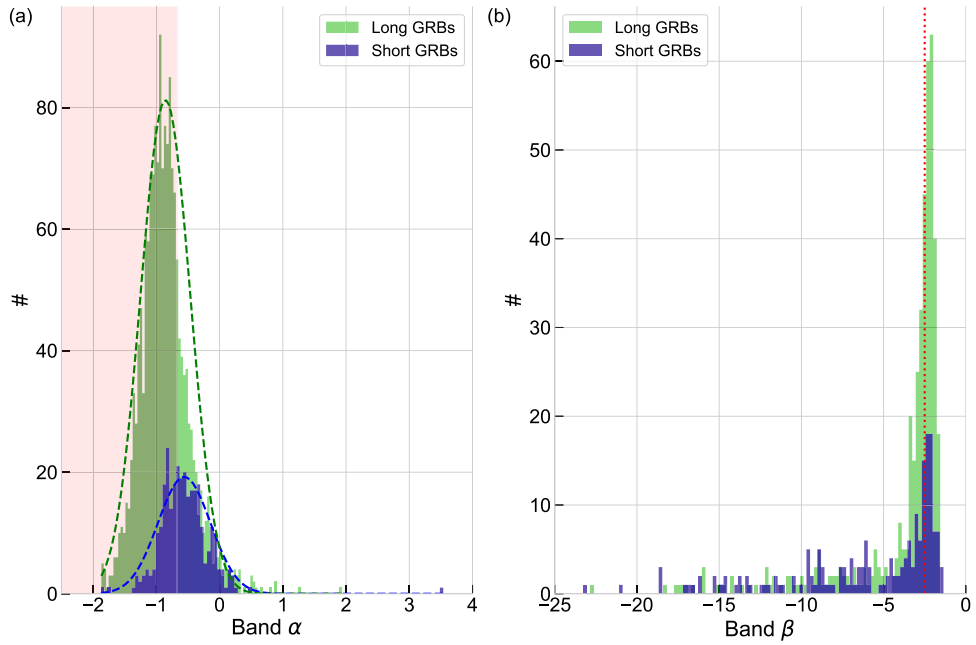

Figure 5. (a) The distribution of well-constrained α values obtained from the Band function fits done to the time-integrated spectra of the *Fermi* detected short GRBs are shown in blue. The shaded region represents the α values that can be produced by simple synchrotron emission. We find 61% of the sample possess α inconsistent with synchrotron emission. (b) The high energy power-law indices, β, of those short GRB spectra inconsistent with $\alpha > -2/3$ are shown in blue. 69% of this distribution is found to possess $\beta < -2.5$ represented by the vertical dotted red line. In both the plots, for comparison, the respective distribution for long GRBs are shown in green (Iyyani & Sharma 2021).

luminosity remains constant within the jet opening angle, θ_j (also see Meng *et al.* 2019). The spectrum of emission from a non-dissipative photosphere would be nearly a blackbody (Pe'er 2008; Beloborodov 2011; Lundman *et al.* 2013). When viewed outside θ_c, the different Lorentz factors would Doppler boost the blackbody temperature to varying temperatures in the observer frame (Figure 6). Thus, the observed spectrum would be a superposition of blackbodies with varying temperatures, thereby softening the low energy part of the spectrum below the spectral peak leading to softer α values than that of a blackbody spectrum when viewed within the jet core ($\alpha > -0.5$) (Lundman *et al.* 2013), see Figure 6.

With this motivations, we analyzed the spectra of 39 short GRBs (sGRB) with known redshifts detected by *Fermi* and Swift until December 2018, using a multi-color blackbody (mBB) model which is later interpreted within the physical scenario described in Lundman *et al.* (2013). We found that 37/39 sGRBs were consistent with mBB model. Among them, using the diagnostic of the expected α for different viewing geometry, we found that 16/37 to be viewed within the jet core and the remaining outside the jet core (Figure 7). Using this inference of viewing geometry and the X-ray afterglow light curve observed by Swift XRT, we estimated the possible range of jet core angle, θ_c, and jet opening angle θ_j. The median values of the cumulative distributions of the probable range of θ_c and θ_j estimated for the different GRBs are found to be 2.6° and 10°, respectively. Thus, our assessments are consistent with the observation of a narrow core region in the jet of GRB170817A. We, thereby, predict that the number of bright sGRBs that can be detected concurrently with gravitational waves will be around 0.19–2.87 events per year for $\theta_c = 2.6°$.

In most spectral analysis studies, we face the issue of degeneracy between various models and in this study, we adopted the methodology of investigating the model of our choice throughout the sample and later assess the feasibility of the inferred physical parameter values. From this method, we find the above physical model of a structured jet of non-dissipative photosphere including viewing geometry can consistently explain the observed sGRB data. This, in turn, suggest that the sGRB jets are likely to be

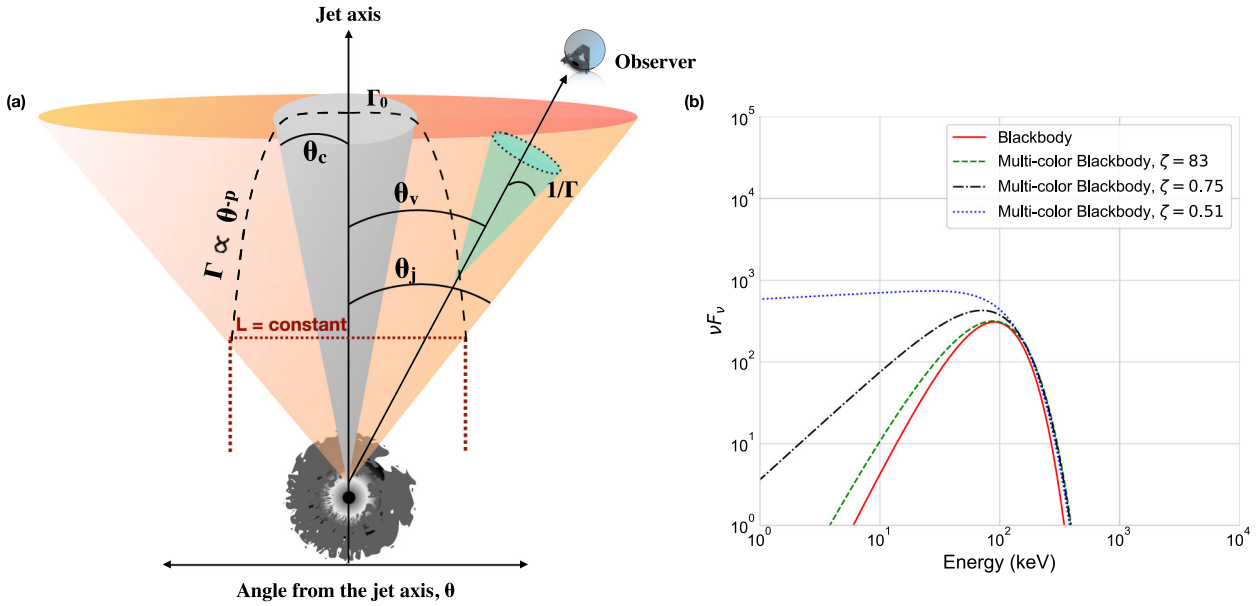

Figure 6. (a) The schematic diagram of the structured jet model considered in Iyyani & Sharma (2021) based on the work of Lundman *et al.* (2013) is shown. The different angles such as jet core (θ_c), jet opening angle (θ_j), viewing angle (θ_v), the viewing cone of $1/\Gamma$ and the angular dependence of the Lorentz factor and jet luminosity profiles are depicted. (b) The multi-color blackbody model for different variations of temperature evolution (represented by ζ, for more details refer Iyyani & Sharma 2021) are shown. For comparison, the blackbody spectrum is shown in a red solid line (Iyyani & Sharma 2021).

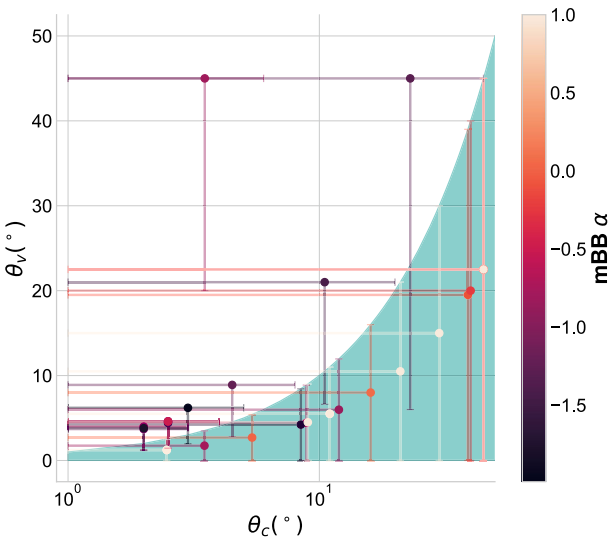

Figure 7. The probable ranges of viewing angle, θ_v versus the jet core, θ_c estimated for the 37 short GRBs in the sample study are shown. The values are color coded with respect to the respective α of the mBB model fits obtained for their GRB spectra.

baryon-dominated which further points to the black hole as the central engine rather than a magnetar which otherwise would have produced a Poynting flux-dominated jet. However, more affirmative conclusions require more investigations using different structured jet models of different compositions and highly sensitive gravitational-wave observations enabling us to determine the post-merger remnant from the detected waveforms.

6. Future outlook

The traditional methodology of spectral analysis has provided us with a wealth of information. However, the evolving and more realistic theories have made the analyzing models highly degenerate and indistinguishable with respect to spectral data. Thereby, more new methodologies involving robust statistical analysis techniques and theories with clear predictions need to be developed and tested against observations. In addition, new observables like polarization and other messengers like gravitational waves and neutrinos are highly promising and provide us better insights and understanding of the various aspects of GRB physics. Thus, the author strongly believe that in the new era of multi-messenger astronomy, gamma-ray bursts hold a huge potential for more breakthrough discoveries.

References

Abbott B. P., Abbott R., Abbott T. D., *et al.* 2017a, ApJL, 848, L13

Abbott B. P., Abbott R., Abbott T. D., *et al.* 2017b, Phys. Rev. Lett., 119, 161101

Acuner Z., Ryde F., Pe'er A., Mortlock D., Ahlgren B. 2020, ApJ, 893, 128

Ahlgren B., Larsson J., Nymark T., Ryde F., Pe'er A. 2015, MNRAS, 454, L31

Ahlgren B., Larsson J., Valan V., *et al.* 2019, ApJ, 880, 76

Alexander K. D., Margutti R., Blanchard P. K., *et al.* 2018, ApJL, 863, L18

Beloborodov A. M. 2010, MNRAS, 407, 1033

Beloborodov A. M. 2011, ApJ, 737, 68

Beniamini P., Barniol Duran R., Giannios D. 2018, MNRAS, 476, 1785

Beniamini P., Giannios D., Metzger B. D. 2017, MNRAS, 472, 3058

Burgess J. M. 2014, arXiv:1408.3973

Burgess J. M., Bégué D., Greiner J., *et al.* 2020, Nat. Astron., 4, 174

Burgess J. M., Preece R. D., *et al.* 2014, ApJ, 784, 17

Cenko S. B., Frail D. A., *et al.* 2011, ApJ, 732, 29

Chakrabarty D. 2008, in American Institute of Physics Conference Series, Vol. 1068, American Institute of Physics Conference Series, eds. Wijnands R., Altamirano D., Soleri P., *et al.* p. 67

Chand V., Chattopadhyay T., Iyyani S., *et al.* 2018, ApJ, 862, 154

Chattopadhyay T., Vadawale S. V., Aarthy E., *et al.* 2017, arXiv:1707.06595

Chattopadhyay T., Vadawale S. V., Aarthy E., *et al.* 2019, ApJ, 884, 123

Chauvin M., Roques J. P., Clark D. J., Jourdain E. 2013, ApJ, 769, 137

Chen W.-X., Beloborodov A. M. 2007, ApJ, 657, 383

Coburn W., Boggs S. E. 2003, Nature, 423, 415

Cucchiara A., Levan A. J., Fox D. B., *et al.* 2011, ApJ, 736, 7

Díaz M. C., Macri L. M., Garcia Lambas D., *et al.* 2017, ApJL, 848, L29

Forot M., Laurent P., Lebrun F., Limousin O. 2007, ApJ, 668, 1259

Gehrels N., Swift 2004, in Bulletin of the American Astronomical Society, Vol. 36, American Astronomical Society Meeting Abstracts, #116.01

Ghirlanda G., Pescalli A., Ghisellini G. 2013, MNRAS, 432, 3237

Gill R., Granot J., Kumar P. 2018, arXiv:1811.11555

Gill R., Kole M., Granot J. 2021, arXiv:2109.03286

Goldstein A., Preece R. D., *et al.* 2013, ApJS, 208, 21

Golkhou V. Z., Butler N. R. 2014, ApJ, 787, 90

Götz D., Laurent P., Lebrun F., Daigne F., Bošnjak Ž. 2009, ApJL, 695, L208

Granot J. 2003, ApJL, 596, L17

Granot J., Gill R., Guetta D., De Colle F. 2018, MNRAS, 481, 1597

Gruber D., Goldstein A., *et al.* 2014, ApJS, 211, 12

Guiriec S., Briggs M. S., *et al.* 2010, ApJ, 725, 225

Haggard D., Nynka M., Ruan J. J., *et al.* 2017, ApJL, 848, L25

Hessels J. W. T., Ransom S. M., Stairs I. H., *et al.* 2006, Science, 311, 1901

Iyyani S., Ryde F., *et al.* 2013, MNRAS, 433, 2739

Iyyani S., Ryde F., Ahlgren B., *et al.* 2015, MNRAS, 450, 1651

Iyyani S., Ryde F., Burgess J. M., Pe'er A., Bégué D. 2016, MNRAS, 456, 2157

Iyyani S. 2018, J. Astrophys. Astron., 39, 75

Iyyani S., Sharma V. 2021, ApJS, 255, 25

Kalemci E., Boggs S., Wunderer C., Jean P. 2004, in ESA Special Publication, Vol. 552, 5th INTEGRAL Workshop on the INTEGRAL Universe, eds. Schoenfelder V., Lichti G., Winkler C., p. 859

Kawabata K. S., Deng J., Wang L., *et al.* 2003, ApJL, 593, L19

Kim S., Schulze S., Resmi L., *et al.* 2017, ApJL, 850, L21

Kole M. 2018, arXiv:1804.04864

Kouveliotou C., Meegan C. A., Fishman G. J., *et al.* 1993, ApJL, 413, L101

Kumar P., Zhang B. 2015, Phys. Rep., 561, 1

Langer N., van Marle A. J., Poelarends A. J. T., Yoon S.-C. 2008, in Astronomical Society of the Pacific Conference Series, Vol. 388, Mass Loss from Stars and the Evolution of Stellar Clusters, eds. de Koter A., Smith L. J., Waters L. B. F. M., p. 37

Larsson J., Racusin J. L., Burgess J. M. 2015, ApJL, 800, L34

Lee H. K., Wijers R. A. M. J., Brown G. E. 2000, Phys. Rep., 325, 83

Leng M., Giannios D. 2014, MNRAS, 445, L1

Lundman C., Pe'er A., Ryde F. 2013, MNRAS, 428, 2430

Lundman C., Pe'er A., Ryde F. 2014, MNRAS, 440, 3292

MacLachlan G. A., Shenoy A., Sonbas E., *et al.* 2013, MNRAS, 432, 857

McConnell M. L., Ryan J. M., Smith D. M., Lin R. P., Emslie A. G. 2002, Sol. Phys., 210, 125

Meegan C., Lichti G., *et al.* 2009, ApJ, 702, 791

Meng Y.-Z., Liu L.-D., Wei J.-J., Wu X.-F., Zhang B.-B. 2019, ApJ, 882, 26

Metzger B., Giannios D., Thompson T., Bucciantini N., Quataert E. 2011, MNRAS, 413, 2031

Metzger B. D. 2017, Living Rev. Relativ., 20, 3

Metzger B. D., Beniamini P., Giannios D. 2018, ApJ, 857, 95

Mooley K. P., Frail D. A., Dobie D., *et al.* 2018a, ApJL, 868, L11

Mooley K. P., Deller A. T., Gottlieb O., *et al.* 2018b, Nature, 561, 355

Narayan R., Piran T., Kumar P. 2001, Astrophys. J., 557, 949

Özel F., Psaltis D., Narayan R., Santos Villarreal A. 2012, ApJ, 757, 55

Paciesas W. S., Pendleton G. N., Lestrade J. P., *et al.* 1989, in Proc. Spie., Vol. 1159, EUV, X-Ray, and Gamma-Ray Instrumentation for Astronomy and Atomic Physics, eds. Hailey C. J., Siegmund O. H. W., p. 156
Patruno A., Haskell B., Andersson N. 2017, ApJ, 850, 106
Pe'er A., Waxman E. 2004, ApJ, 613, 448
Pe'er A. 2008, ApJ, 682, 463
Pe'er A. 2015, Adv. Astron., 2015, 907321
Pian E., D'Avanzo P., Benetti S., *et al.* 2017, Nature, 551, 67
Preece R. D., Briggs M. S., *et al.* 1998, ApJL, 506, L23
Rao A. R., Bhattacharya D., Bhalerao V. B., Vadawale S. V., Sreekumar S. 2017, arXiv:1710.10773
Rees M. J., Meszaros P. 1992, MNRAS, 258, 41P
Resmi L., Schulze S., Ishwara-Chandra C. H., *et al.* 2018, ApJ, 867, 57
Rowlinson A., Gompertz B. P., Dainotti M., *et al.* 2014, MNRAS, 443, 1779
Ruffert M., Janka H. T., Takahashi K., Schaefer G. 1997, AAP, 319, 122
Ryde F. 2004, ApJ, 614, 827
Ryde F., Pe'er A. 2009, ApJ, 702, 1211
Sarin N., Lasky P. D., Ashton G. 2019, ApJ, 872, 114
Schönfelder V., Bennett K., Bloemen H., *et al.* 1993, Adv. Space Res., 13, https://doi.org/10.1016/0273-1177(93)90176-C
Sharma V., Iyyani S., Bhattacharya D., *et al.* 2019, ApJL, 882, L10
Sharma V., Iyyani S., Bhattacharya D., *et al.* 2020, Mon. Notices R. Astron. Soc., 493, 5218
Sharma V., Iyyani S., Bhattacharya D. 2021, ApJL, 908, L2
Stanek K. Z., Matheson T., Garnavich P. M., *et al.* 2003, ApJL, 591, L17
Tavani M. 1996, ApJ, 466, 768
Tchekhovskoy A., Narayan R., McKinney J. C. 2011, MNRAS, 418, L79
Toma K., Sakamoto T., Zhang B., *et al.* 2009, ApJ, 698, 1042
Troja E., Piro L., Ryan G., *et al.* 2018, MNRAS, 478, L18
Usov V. V. 1992, Nature, 357, 472
Wigger C., Hajdas W., Arzner K., Güdel M., Zehnder A. 2004, ApJ, 613, 1088
Woosley S. 1993, Astrophys. J., 405, 273
Yonetoku D., Murakami T., Gunji S., *et al.* 2011, ApJL, 743, L30
Yonetoku D., Murakami T., Gunji S., *et al.* 2012, ApJL, 758, L1
Zhang B., Yan H. 2011, ApJ, 726, 90
Zhang S.-N., Kole M., Bao T.-W., *et al.* 2019, Nat. Astron., 3, 258
Zhao L., Liu L., Gao H., *et al.* 2020, ApJ, 896, 42